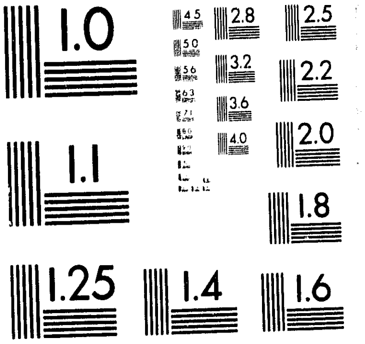
1.0
4.5
5.0
5.6
6.3
7.1
8.0
2.8
3.2
3.6
4.0
2.5
2.2
2.0
1.1
1.8
1.25
1.4
1.6

1 of 1

Conf-930405--44

UCRL-JC-114157
PREPRINT

RECEIVED
OCT 14 1993
OSTI

Using the Rule of Mixtures to Examine the Hardness of Cu/Cu-Zr Multilayers

T. P. Weihs, T. W. Barbee, Jr. and M. A. Wall

This paper was prepared for submittal to the 1993 Materials Research Society Spring Meeting Symposium M-1, San Francisco, CA, April 12-16, 1993.

June 1993

Lawrence
Livermore
National
Laboratory

MASTER

ds

DISTRIBUTION OF THIS DOCUMENT IS UNLIMITED

USING THE RULE OF MIXTURES TO EXAMINE THE HARDNESS OF Cu/Cu-Zr MULTILAYERS

T.P.Weihs, T.W. Barbee, Jr., and M.A. Wall, Lawrence Livermore National Laboratory,
Livermore, CA 94550

ABSTRACT

Cu/Cu-Zr multilayer foils were fabricated and indented to determine the degree to which multilayer hardness is enhanced by increasing the volume fraction of the harder phase. Using sputter deposition and thermal processing a series of foils was fabricated in which the thicknesses of the Cu layers remained fixed while the thicknesses of the alternate Cu-Zr layers varied. These samples were then indented both parallel and normal to their layering. In general, hardness increased as the volume fraction of the harder Cu-Zr phase rose. When the films were loaded parallel to their layering, the measured hardnesses were higher and the dependencies on volume fraction of the Cu-Zr phase were stronger than when the films were loaded normal to their layering. These results agree with predictions based on isostress and isostrain theories. The relationships between hardness and volume fraction are used to compare the hardnesses of the Cu-Zr phases: amorphous Cu-Zr, $Cu_{51}Zr_{14}$ and Cu_9Zr_2, and to show that the hardness of the textured, as-deposited Zr layers is highly anisotropic .

INTRODUCTION

The ability to harden a multilayered film by decreasing its bilayer thicknesses has been studied extensively [1-4]. Many researchers have reported substantial increases in hardness for a wide variety of thicknesses and a wide variety of materials. However, throughout this work, little attention has been given to the volume fraction of the different materials in a multilayer system. We suggest that volume fraction deserves greater consideration as multilayered films are being developed for protective coating applications. This geometrical parameter will be an important design tool as engineers attempt to optimize several film properties such as wear resistance, fracture resistance and corrosion resistance in a single multilayered coating. Here, we determine the change in hardness of Cu/Cu-Zr multilayer foils as the volume fraction of the harder Cu-Zr phase is increased. To isolate the effect of volume fraction from other hardening effects, the foils were deposited and then processed to produce a set of specimens in which the thickness of the softer Cu layers remained fixed, while the thickness of the harder Cu-Zr layers increased. Under these conditions, the volume fraction of the stronger Cu-Zr phase was increased without enhancing the hardness of either individual layer by decreasing its thickness. In this case, any enhancements in the multilayer's hardness are due to an increase in the volume fraction of the harder Cu-Zr phase and not a reduction in layer thickness.

THEORY

When one compresses a layered composite normal to its layering, isostress conditions exist, and the weakest layer determines the yield load of the composite [5]. In contrast, when a layered composite is compressed parallel to its layering, isostrain conditions exist and the volume fraction and the flow behavior of each layer determine the deformation of the composite [5]. If similar loading conditions exist during the indentation of multilayers, then the foil's hardness, H, would equal the hardness of the weakest layer when indenting normal to the layering

$$H = H_A \tag{1}$$

and it would follow the rule of mixtures when indenting parallel to the layering,

$$H = X_A*H_A + X_B*H_B \tag{2}$$

where X_A and X_B are volume fractions of layers A and B, and H_A and H_B are their individual layer hardnesses. The deformation under pointed or rounded indenters, however, is radial in nature and not uniaxial [6]. Pure isostress and pure isostrain conditions do not exist during such tests. Consequently, a multilayered foil will be harder than its weakest layer when indenting normal to its layering, and it will be softer than the rule of mixtures suggests when indenting parallel to its layering. The goal here is to show that some rule of mixtures, in which volume fraction and layer hardness are considered, can be applied to both "isostress" and "isostrain" indentations of multilayered foils. The strength of the dependence on volume fraction will simply vary with the loading geometry.

We begin by defining the simple relation between volume fraction and layer thickness for a multilayer of alternate layers of A and B. The volume fractions, X_A and X_B, are given by

$$X_A = t_A/(t_A + t_B) \quad \text{and} \quad X_B = t_B/(t_A + t_B) \qquad (3)\ \&\ (4)$$

where t_A and t_B are the thicknesses of layer A and B. Note that one can not change the volume fraction without changing the thickness of at least one of the two layers. Next, we consider the relationship between a layer's hardness and its thickness,

$$H_A = H_{Ao} + K_A{*}t_A^{-n} \qquad \text{and} \qquad H_B = H_{Bo} + K_B{*}t_B^{-n} \qquad (5)\ \&\ (6)$$

In Equations (5) and (6), H_{Ao} and H_{Bo} are constant terms that do not scale with layer thickness. They depend only on the resistance to deformation that is offered by the phase itself in an infinitely thick layer or grain. $K_A{*}t^{-n}$ and $K_B{*}t^{-n}$ account for the hardening that is produced by the reduction in layer thickness. K_A and K_B are constants, and n varies from 0.5 for Hall-Petch type strengthening [7] to 1.0 for a strengthening mechanism such as modulus hardening [8]. Combining Equations (5) and (6) into the standard rule of mixtures [5] in Equation (2) yields

$$H = X_A{*}(H^0_A + K_A{*}t_A^{-n}) + X_B{*}(H^0_B + K_B{*}t_B^{-n}) \qquad (7)$$

or

$$H = (H^0_A + K_A{*}t_A^{-n}) + X_B{*}[(H^0_B + K_B{*}t_B^{-n}) - (H^0_A + K_A{*}t_A^{-n})] \qquad (8)$$

To assess the dependence of hardness on the volume fraction of each phase, we hold the thickness of the softer (Cu) A layer constant and increase the thickness of the harder (Cu-Zr) B layer. Under these conditions, the hardness of layer A will remain constant (Equation (5)) while the hardness of layer B will decrease (Equation (6)). However, the decrease in H_B should be small because the amorphous or intermetallic Cu-Zr phases in the B layers are inherently hard, [9,10] and layer thickness should not affect their resistance to plastic deformation significantly. Based on these predictions, the three separate terms in parenthesis in Equation (8) will be relatively constant, and the Cu/Cu-Zr multilayer hardness, H, should vary linearly with X_B. Any enhancements in the hardness of the Cu/Cu-Zr foils as X_B and t_B increase will be due solely to a change in the volume fraction of Cu-Zr and not a reduction in the thickness of either layer.

EXPERIMENTAL PROCEDURES

A series of Cu/Cu-Zr multilayered foils was produced by depositing and processing alternate layers of Cu and Zr. The foils were magnetron sputter deposited onto 3.0in and 6.0in (100) Si wafers at powers ranging from 41W to 645W. After deposition, the multilayers were removed from their substrates and cut into specimens with 6mm diameters. Since the as-deposited foils were approximately 26μm thick, the specimens were easily handled as free-standing samples. The as-deposited layered structure of the Cu/Zr samples is shown in Figure 1(a). The Cu layers are polycrystalline, and the width of the Cu grains scale with their layer thickness. The Zr layers are also polycrystalline, but some solid state amorphization (SSA) [11] occurs in these layers during deposition and can be easily observed at higher magnifications. Isochronal and isothermal DSC scans were used to thermally process these multilayers and thereby change both the composition and the structure of the thinner Zr layers. In all such scans, the 6mm specimens were crimped in Cu pans and were heated in a DSC chamber which was purged continuously with Ar. Data for isochronal scans of four sample sets is shown in Figure 2. The three exotherms that are clearly visible correspond to the transformation of a fraction of each Cu layer and all of each Zr layer into three different phases: an amorphous Cu-Zr alloy (aCu-Zr), the crystalline alloy $Cu_{51}Zr_{14}$, and finally the stable crystalline alloy Cu_9Zr_2. After determining the temperatures at which each phase formed, the samples were scanned to those temperatures and then quenched to produce two new layered structures: Cu/aCu-Zr and Cu/$Cu_{51}Zr_{14}$. The thicknesses of the Cu and Cu-Zr layers are based on reported compositions of aCu-Zr [12] and $Cu_{51}Zr_{14}$ [13], and are listed in Table 1 along with the as-deposited Cu and Zr layer thicknesses. Note that the Cu layer thicknesses are relatively constant in the processed specimens. Since Reactions 1 and 2 overlap in Figure 2, some foils were isothermally annealed at 310°C for 200min to insure completion of the SSA without nucleation of the crystalline phase, $Cu_{51}Zr_{14}$. However, these specimens were only indented on edge since their surfaces were partially oxidized after such long anneals. During the third reaction in Figure 2, the layering broke down and the Cu_9Zr_2 grains grew significantly, encompassing the smaller Cu grains. This final structure is shown in a TEM micrograph in Figure 1(b). A detailed analysis of the thermal processing of the Cu/Cu-Zr foils is given in reference [14].

Table 1: Layer and Film Thicknesses for As-Deposited and Processed Samples

		As-Deposited		Post Reaction 1		Post Reaction 2		
Sample Set	% Zr	Cu (Å)	Zr (Å)	Cu (Å)	aCu-Zr (Å)	Cu (Å)	$Cu_{51}Zr_{14}$ (Å)	Film (μm)
A	3.09	387.3	24.5	350.2	56.8	342.2	68.2	25.7
B	5.52	424.9	49.2	350.4	114.1	334.4	136.9	26.5
C	7.38	467.4	73.9	355.6	171.2	331.7	205.5	27.1
D	9.00	502.5	98.5	353.4	228.4	321.4	274.1	27.4

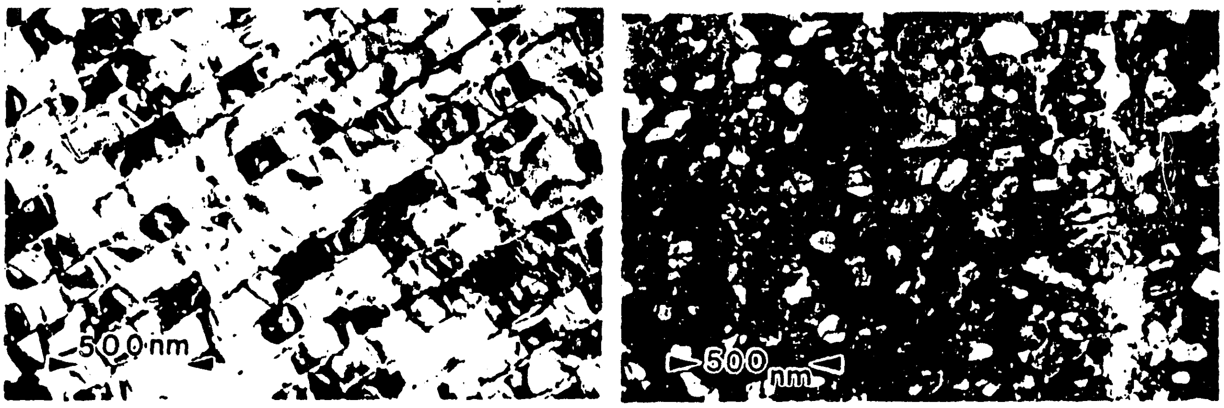

Figure 1: The TEM images show polycrystalline Cu layered with polycrystalline Zr in (a) and Cu grains imbedded in Cu_9Zr_2 grains in (b).

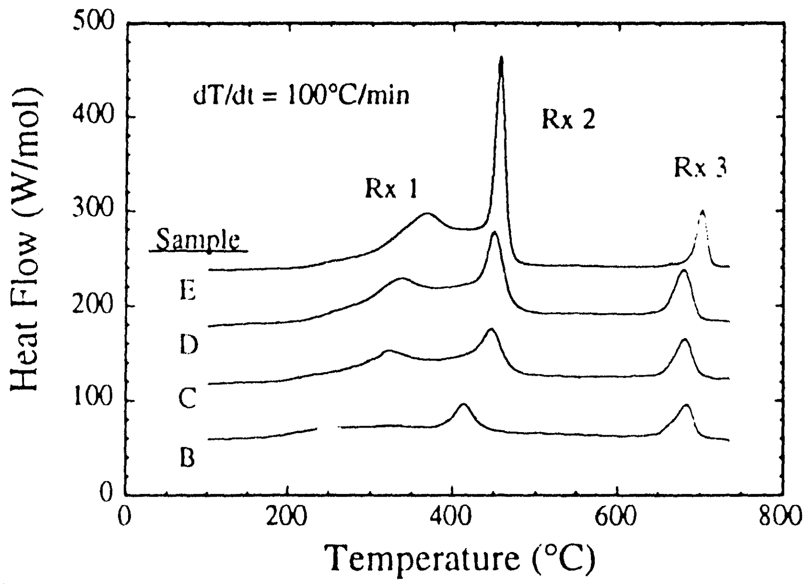

Figure 2: Isochronal DSC scans of the 4 Samples listed in Table 1. The heating rate was 100°C/min.

The different phases in the processed films were determined using X-ray diffraction (XRD) and transmission electron microscopy (TEM). The Cu and the Zr layers were highly textured as deposited. The stable Cu phase retained this texture during all thermal processing. Low-angle XRD and cross-sectional TEM confirmed the presence and the uniformity of layering within samples that were heated up to 650°C. For mechanical characterizations, 6mm disks were glued to glass substrates to measure hardnesses normal to the layers. Similar specimens were mounted on edge in epoxy and then mechanically polished to measure hardnesses parallel to the layers. For each sample set, four different specimens were considered - Cu/Zr, Cu/aCu-Zr, Cu/$Cu_{51}Zr_{14}$ and Cu in Cu_9Zr_2. All hardness measurements were performed at room temperature with a Vickers Hardness Tester and a 10g load.

RESULTS AND DISCUSSION

After the Zr in the multilayers reacted with the surrounding Cu and formed amorphous Cu-Zr, and then crystalline $Cu_{51}Zr_{14}$, the hardness of each sample increased as shown in Figure 3. The percentage increase was largest for Sample D which contains the largest volume fraction of the Cu-Zr phase. When specimens were scanned above 650°C, the stable phase, Cu_9Zr_2, nucleated, the layered structure broke down, and the measured hardnesses decreased significantly. These large decreases are attributed to the loss of the layered structure.

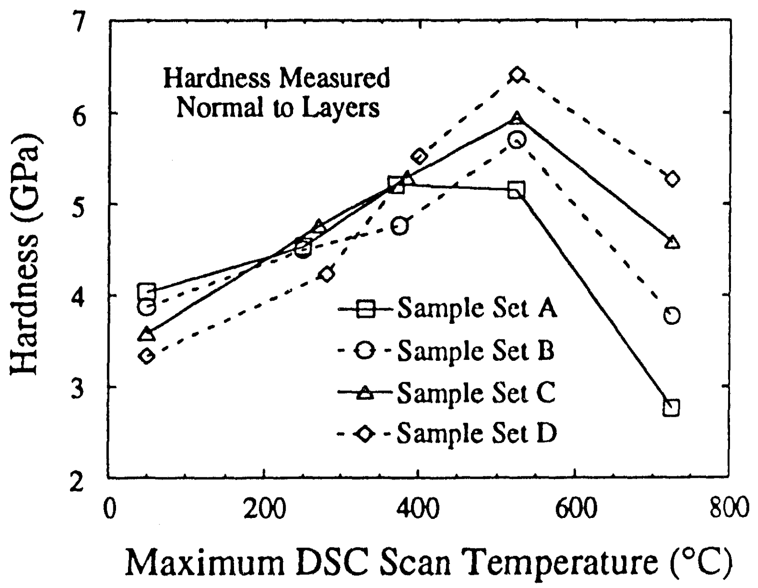

Figure 3: The hardness of each specimen is plotted versus the temperature to which it was scanned in a DSC.

In Figures 4 and 5, the hardnesses of the Cu-Zr foils are plotted as a function of volume fraction for both loading geometries. The data in Figure 4 is taken from indentations made normal to the foil layering and the data in Figure 5 is taken from indentations made parallel to the foil layering. The results for the four individual foil structures - Cu/Zr, Cu/aCu-Zr, Cu/$Cu_{51}Zr_{15}$, and Cu in Cu_9Zr_2 will be reviewed first, and then the general trends of the collective data set shall be considered.

For the as-deposited foils with the Cu/Zr structure, the dependence of hardness on volume fraction differs dramatically between the two loading geometries. As the volume fraction of Zr rises, the as-deposited hardnesses decrease in Figure 4 and increase in Figure 5. The opposite dependence is attributed to the texturing of the Zr and the nature of deformation in hexagonal close-packed (HCP) crystals [9]. After deposition, the Zr in the multilayered foils is highly textured with its basal planes lying in the plane of the foil. When HCP crystals such as Zr are indented, hardness varies considerably with crystallographic orientation. The hardness measured on the basal plane of Ti [15], Co [16], Re [17] or Zn [15] differs from the hardness measured on {1120} planes of these crystals by a factor of up to 5. The direction of this difference, whether 1 to 5 or 5 to 1, can vary as well. We suggest that the highly textured Zr layers show similar anisotropy. When the as-deposited foils are indented normal to their layering, the Zr deforms more easily than the Cu and therefore reduces the foil hardness as its volume fraction increases in Figure 4. When the as-deposited foils are indented parallel to their layering, the Zr deforms less easily than the Cu and thereby raises the foil hardness as its volume fraction increases in Figure 5. For Sample Set D with 9.0 at% Zr, this anisotropy produces a 33% difference between the hardnesses measured in the two loading geometries. Such anisotropies must be considered when designing multilayered coatings.

After the Cu-Zr multilayers were processed to obtain the Cu/aCu-Zr and the Cu/$Cu_{51}Zr_{14}$ structures, with constant Cu layer thicknesses, the measured hardnesses showed a consistent increase with the volume fraction of the Cu-Zr phase under both loading geometries. In Figure

4, the dependence of hardness on volume fraction is weak for this "isostress" type of loading, particularly for the Cu/aCu-Zr foils. In Figure 5, the dependence is much stronger as the loading approaches an isostrain type of geometry. For the Cu/$Cu_{51}Zr_{14}$ foils indented parallel to their layering, hardness increases 150% as the volume fraction of Cu-Zr varies from 0.0 to 1.0 in Figure 5. While this percentage increase could be larger under pure isostrain conditions, it does imply a strong dependence of multilayer hardness on volume fraction. It is important to remember that for these specimens, all of the increases in hardness are attributed to a change in volume fraction and not to a reduction in layer thickness. According to Equations (5) and (6), the individual Cu layers should have a constant hardness since their thicknesses does not vary. The individual Cu-Zr layers could actually decrease in hardness because their thicknesses quadruple. According to Equation (8), the thickening of the Cu-Zr layers could cause the positive slopes in Figures 4 and 5 to decrease as $X_{Cu\text{-}Zr}$ increases. The lack of any appreciable decreases of slopes in either figure suggests that the hardnesses of aCu-Zr and $Cu_{51}Zr_{14}$ are not strongly dependent on their layer thicknesses.

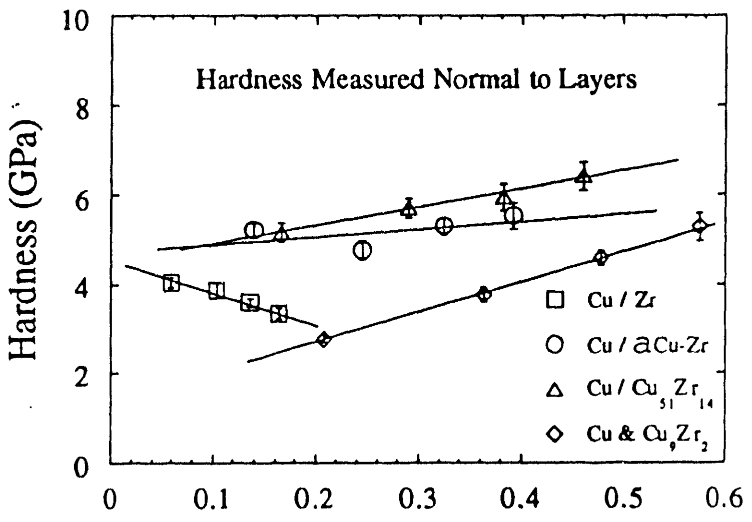

Figure 4: Hardness of Cu-Zr multilayer foils measured normal to their layering with a 10g load.

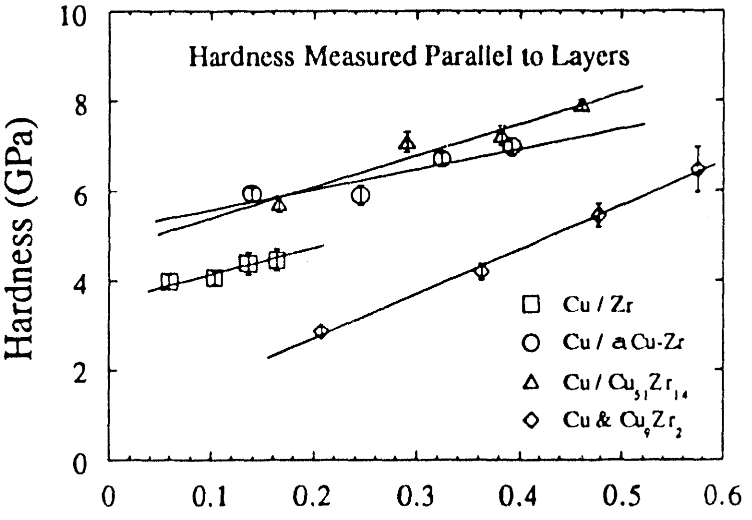

Figure 5: Hardness of Cu-Zr multilayer foils measured parallel to their layering with a 10g load.

The final data set consists of specimens with clumps of small Cu grains embedded in larger Cu_9Zr_2 grains (Figure 1(b)). These non-layered, particle-like composite foils are generally softer than the corresponding layered structures. Their hardness data produce the best linear fit of all the specimen sets in Figure 4 and 5 and is readily described by the simple rule of mixtures in Equations (2). However, the foils are not isotropic since hardness varies more rapidly with Cu-Zr volume fraction in Figure 5 than in Figure 4. As $X_{Cu\text{-}Zr}$ increases from 0.0 to 0.6 in Figure 5, the hardness of the foils increases by a factor of 8. Using the extrapolated values at $X_{Cu\text{-}Zr} = 1.0$ in Figure 5, the hardness of Cu_9Zr_2 (10.6GPa) is only 10% less than that estimated for $Cu_{51}Zr_{14}$ (11.7GPa) at $X_{Cu\text{-}Zr} = 1.0$. This 10% difference matches the percentage difference measured on bulk samples [10] almost exactly. The hardness of the Cu phase, measured at $X_{Cu\text{-}Zr} = 0.0$, appears to decrease significantly after the final reaction and the breakdown of layering. Some of this decrease could be attributed to the stacking of the Cu grains that is seen in Figure 1(b). If the stacking enables dislocations to move readily from one Cu grain to the next, then the effective Cu grain size is much larger than the grain size seen in the layered foils (Figure 1(a), and the effective hardness of the Cu volume decreases.

Referring now to the processed specimens in general, the average foil hardness increases as the volume fraction of the harder Cu-Zr phase rises in Figures 4 and 5. This result shows no evidence of a purely isostress condition during multilayer indentation. The softer phase in a bilayered foil does not strictly determine the multilayer hardness, even when indenting normal to the layering. The results do show that the hardness of a multilayer foil follows a general rule of mixtures that accounts for the hardness and the volume fraction of each phase. The dependence of hardness on volume fraction is stronger when indenting parallel to the foil layering than when indenting normal to the foil layering for all of the processed foils. This difference is shown by the sharper rise of data in Figure 5 than in Figure 4, and it agrees with earlier predictions. If a modified rule of mixtures can be determined for several Cu layer thicknesses, volume fractions and loading geometries, then one could begin to predict multilayer hardnesses for any combination of layer thicknesses, volume fractions or loading geometries.

CONCLUSIONS

The hardness of Cu/Cu-Zr multilayered foils increases as the volume fraction of the Cu-Zr layers rises. This dependence can be modeled using a modified rule of mixtures. When the foils are loaded parallel to their layering, the foils are harder and depend more strongly on volume fraction than when the foils are loaded normal to their layering. This result agrees with predictions based on isostress and isostrain theories, and it suggests that one can predict the hardness of multilayered foils using volume fractions, loading geometry and a modified rule of mixtures. Using the linear variations of the measured data, the hardness of the individual phases - Cu, aCu-Zr, $Cu_{51}Zr_{14}$ and Cu_9Zr_2 - were compared and the hardness of the textured Zr layers was shown to be highly anisotropic.

ACKNOWLEDGMENTS

The authors gratefully acknowledge the help of J. Furr, J. Schimmeyer and B. Viani. This work was performed under the auspices of the US Department of Energy by the Lawrence Livermore National Laboratory under contract #W-7405-ENG-48.

REFERENCES

1) T. Foecke and D.S. Lashmore, Scripta Met., **27**, 651 (1992).
2) K.K. Shih and D.B. Dove, Appl. Phys. Let., 61, 654 (1992).
3) P.B. Mirkarimi, L. Hultman and S.A. Barnett, Appl. Phys. Let., **57**, 2654 (1990).
4) R.C. Cammarata, T.E. Schlesinger, C. Kim, S.B. Qadri and A.S. Edelstein, Appl. Phys. Lett., **56**, 1862 (1990).
5) C. R. Barnett, W.D. Nix and A.S. Tetelman, The Principles of Engineering Materials, pp. 318-20, Prentice-Hall, Inc., NJ (1973).
6) D. Tabor, The Hardness of Metals, Oxford (1951).
7) E.O. Hall, Proc Phys. Soc., Lond., **B64**, 747 (1951); N.J. Petch, J. Iron & Steel, **174**, 25 (1953).
8) J.S. Koehler, Phys. Rev. B, **2**, 547 (1970) and S.L. Lehoczky, Phys. Rev. Lett., **41**, 1814 (1978).
9) G.E. Dieter, Mechanical Metallurgy, p. 37, McGraw-Hill, N.Y. (1976).
10) J.L Glimois, P. Forey and J.L. Feron, J. Less-Common Met., **113**, 213 (1985).
11) W.L Johnson, Mater. Sci. Eng., **97**, 1 (1988).
12) T.W. Barbee, Jr., R.G. Walmsley, A.F. Marshall, D.L. Keith, and D.A. Stevenson, Appl. Phys. Lett., **38**, 132 (1981).
13) E. Kneller, Y. Khan, and U. Gorres, Z. Metallkd., **77**, 43 (1986).
14) T.P. Weihs, T.W. Barbee, Jr., and M.A. Wall, Proceedings of Symposium O, "Phase Transformations in Thin Films," MRS Meeting, Spring 1993.
15) H. O'Neill, Hardness Measurements of Metals and Alloys, pp. 77-78, Chapman and Hall, LTD, UK (1967).
16) F. R. Moral, J. Metals, **10**, 662 (1958).
17) A. Lawley and R. Maddin, Acta Met., **8**, 275 (1960).

DATE FILMED

12/10/93

END